J Neurophysiol 91: 78–91, 2004.
First published October 1, 2003; 10.1152/jn.00741.2003.

Long-Lasting Activation of Rhythmic Neuronal Activity by a Novel Mechanosensory System in the Crustacean Stomatogastric Nervous System

Mark P. Beenhakker, Dawn M. Blitz, and Michael P. Nusbaum
Department of Neuroscience, University of Pennsylvania School of Medicine, Philadelphia, Pennsylvania 19104

Submitted 31 July 2003; accepted in final form 22 September 2003

Beenhakker, Mark P., Dawn M. Blitz, and Michael P. Nusbaum. Long-lasting activation of rhythmic neuronal activity by a novel mechanosensory system in the crustacean stomatogastric nervous system. *J Neurophysiol* 91: 78–91, 2004. First published October 1, 2003; 10.1152/jn.00741.2003. Sensory neurons enable neural circuits to generate behaviors appropriate for the current environmental situation. Here, we characterize the actions of a population (about 60) of bilaterally symmetric bipolar neurons identified within the inner wall of the cardiac gutter, a foregut structure in the crab *Cancer borealis*. These neurons, called the ventral cardiac neurons (VCNs), project their axons through the crab stomatogastric nervous system to influence neural circuits associated with feeding. Brief pressure application to the cardiac gutter transiently modulated the filtering motor pattern (pyloric rhythm) generated by the pyloric circuit within the stomatogastric ganglion (STG). This modulation included an increased speed of the pyloric rhythm and a concomitant decrease in the activity of the lateral pyloric neuron. Furthermore, 2 min of rhythmic pressure application to the cardiac gutter elicited a chewing motor pattern (gastric mill rhythm) generated by the gastric mill circuit in the STG that persisted for $\leq$30 min. These sensory actions on the pyloric and gastric mill circuits were mimicked by either ventral cardiac nerve or dorsal posterior esophageal nerve stimulation. VCN actions on the STG circuits required the activation of projection neurons in the commissural ganglia. A subset of the VCN actions on these projection neurons appeared to be direct and cholinergic. We propose that the VCN neurons are mechanoreceptors that are activated when food stored in the foregut applies an outward force, leading to the long-lasting activation of projection neurons required to initiate chewing and modify the filtering of chewed food.

INTRODUCTION

Sensory systems provide animals with important information that enables the generation of appropriate behaviors (Harris-Warrick and Sparks 1995; Marder and Pearson 1998; McCrea 1998; Pearson 1995, 2001; Pearson et al. 1998; Stein et al. 1997). Sensory neurons that are responsible for mechanoreception are sensitive to distortions of the body caused by either internally or externally generated mechanical energy and thus can sense gravity, pressure, touch, stretch, and vibration (McIver 1985). With respect to rhythmically active neural networks [i.e., central pattern generators (CPGs)] such as those responsible for locomotion, respiration, and feeding, mechanoreceptors are classically thought to provide transient feedback, correctional information used to ensure that the network output is appropriate for the current environmental situation (Stein et al. 1997). In this context, mechanoreceptors regulate, on a cycle-to-cycle basis, the frequency of network activity and the intensity/timing of impulse bursts produced by network neurons.

Phasic regulation of pattern-generating circuits has been well studied in a variety of systems, including feeding in *Aplysia* (Cropper et al. 1996; Evans and Cropper 1998; Evans et al. 1999), flight in locust (Pearson and Wolf 1987, 1988; Pearson et al. 1983; Stein et al. 1997; Wilson 1961; Wolf and Pearson 1987, 1988), swimming in lamprey (Wallen 1982), respiration in rat (Mellen and Feldman 2001), and walking in stick insects (Akay et al. 2001; Hess and Buschges 1999) and cats (Andersson and Grillner 1981; Duysens and Pearson 1980; Duysens et al. 2000; Hiebert et al. 1996; Lam and Pearson 2001; Whelan et al. 1995). Considerable progress has been made in gaining a cellular-level understanding of how these phasic actions are exerted. Work with several systems has established that these types of sensory neurons can also have longer lasting, modulatory actions that reconfigure network dynamics to produce different activity patterns that outlast sensory activation by many cycles (Hooper et al. 1990; Katz and Harris-Warrick 1989; Katz et al. 1989; Sigvardt and Mulloney 1982). In some cases, mechanoreceptor activation can also initiate or terminate network output (Boothby and Roberts 1992; Perrins et al. 2002; Viana di Prisco et al. 1997, 2000).

In this study, we establish the influence of a mechanoreceptive system with both short- and long-lasting actions in the stomatogastric nervous system (STNS) of the crab *Cancer borealis*. The crustacean STNS is an extensively characterized model system for studying rhythmically active neural circuits at the cellular level (Harris-Warrick et al. 1992; Marder and Calabrese 1996; Nusbaum and Beenhakker 2002). The STNS is an extension of the crustacean CNS that contains motor circuits controlling the movement of food through the crab esophagus and 3-compartment stomach (cardiac sac, gastric mill, pylorus). The STNS consists of 4 ganglia, including the paired commissural ganglia (CoGs: about 500 neurons each), the unpaired esophageal ganglion (OG: 14 neurons), and the stomatogastric ganglion (STG: 26 neurons). Most of the STG neurons participate in one or both of 2 well-characterized CPG circuits that generate the gastric mill (food chewing) and pyloric (food filtering) rhythmic motor patterns (Weimann and Marder 1994). In vivo and in vitro, the pyloric circuit is generally spontaneously active, whereas the gastric mill circuit is inactive except when it receives input from specific CoG projection neurons that are not spontaneously active (Blitz and Nusbaum 1997; Blitz et al. 1999; Clemens et al. 1998). The STG circuits can generate many versions of the pyloric and

Address for reprint requests and other correspondence: M. P. Nusbaum, Department of Neuroscience, University of Pennsylvania School of Medicine, 215 Stemmler Hall, Philadelphia, PA 19104-6074 (E-mail: nusbaum@mail.med.upenn.edu).

The costs of publication of this article were defrayed in part by the payment of page charges. The article must therefore be hereby marked "*advertisement*" in accordance with 18 U.S.C. Section 1734 solely to indicate this fact.

gastric mill rhythms (Nusbaum and Beenhakker 2002; Nusbaum et al. 2001). This flexibility results from the synaptic and modulatory actions of projection (Nusbaum et al. 2001) and sensory neurons (Combes et al. 1999; Hooper et al. 1990; Katz and Harris-Warrick 1989; Simmers and Moulins 1988a,b). In *C. borealis*, there are fewer than 20 projection neurons innervating the STG (Coleman et al. 1992).

In the current study we examined the actions of the ventral cardiac neurons (VCNs), a population of mechanosensory neurons in *C. borealis* that modulate the ongoing pyloric rhythm and evoke a long-lasting activation of the gastric mill rhythm. Here, we characterize these events and determine the pathways by which this sensory system activates the gastric mill rhythm. This activation of the gastric mill rhythm by VCN stimulation appears to operate by long-lasting VCN actions on identified projection neurons that are known to activate this motor pattern. Part of this work appeared previously in abstract form (Beenhakker et al. 2000).

METHODS

Animals

Jonah crabs (*Cancer borealis*) were obtained from a commercial supplier (Commercial Lobster and Seafood, Boston, MA) and from the Marine Biological Laboratory (MBL, Woods Hole, MA). Before experimentation, the crabs were housed in commercial tanks containing recirculating, aerated artificial seawater (10–12°C). Before dissection, the crabs were cold-anesthetized by packing them in ice for 30 min. The foregut was then removed and maintained in chilled physiological saline while the STNS was dissected away (Fig. 1*A*).

Solutions

Under most experimental conditions, the STNS was maintained in physiological saline containing (in mM) 440 NaCl, 26 $MgCl_2$, 11 KCl, 13 $CaCl_2$, 10 Trizma base, and 5 maleic acid (pH 7.4–7.6). To limit neuronal interactions to those that were likely to be monosynaptic, in a subset of experiments we superfused the preparation with saline containing 5 times the normal concentration of the divalent salts (i.e., "high-divalent cation saline") (Blitz and Nusbaum 1999). This saline contained (in mM) 439 NaCl, 130 $MgCl_2$, 11 KCl, 64.5 $CaCl_2$, 10 Trizma base, and 5 maleic acid (pH 7.4–7.6). In a few preparations, chemical transmission was eliminated by superfusing the preparation with saline that contained reduced (0.1× normal) concentrations of Ca^{2+} plus a compensatory concentration of Mn^{2+} (i.e., "low-calcium saline") (Blitz and Nusbaum 1997) (in mM): 439 NaCl, 26 $MgCl_2$, 11 KCl, 1.3 $CaCl_2$, 11.7 $MnCl_2$, 10 Trizma base, and 5 maleic acid (pH 7.4–7.6).

In some experiments, neurotransmitter receptor antagonists were superfused to characterize the central actions of the VCN neurons in the CoG. Antagonists used included the serotonin receptor antagonists cinanserin (10^{-4}–10^{-3} M, Tocris Cookson, Ellisville, MO) and atropine (10^{-4} M, Sigma, St. Louis, MO), the nicotinic acetylcholine receptor antagonist decamethonium bromide (10^{-3} M, Sigma), and the muscarinic cholinergic receptor antagonists scopolamine (10^{-4} M, Sigma) and atropine (10^{-3} M).

Electrophysiology

All experiments were performed using either the completely isolated STNS (Fig. 1*B*) or a semi-intact preparation consisting of the isolated STNS attached to a small portion of the cardiac sac containing the cardiac gutter. Both preparations were pinned down in a saline-filled silicone elastomer-lined petri dish (Sylgard 184, KR Anderson, Santa Clara, CA) and superfused continuously (7–12 ml/min) with physiological and/or experimental (high-divalent cation or low-calcium) saline (10–12°C). Intracellular and extracellular recordings of the gastric mill and pyloric rhythms were made using routine methods for the STNS (Fig. 1*C*) (Blitz and Nusbaum 1999). Intracellular recordings were made with Axoclamp 2B amplifiers (Axon Instruments, Foster City, CA) and glass microelectrodes (15–30 MΩ) filled with 4 M potassium acetate and 20 mM KCl. Intracellular current injections were performed in single electrode discontinuous current clamp mode with sample rates of 2–3 kHz. To facilitate intracellular recordings, the STNS ganglia were desheathed and illuminated with light transmitted through a dark-field condenser (Nikon, Tokyo, Japan). Extracellular recordings were made by placing a reference wire electrode (stainless steel) in the bath and a recording wire alongside an individual nerve and isolated from the bath by petroleum jelly (Vaseline, Chesebrough-Ponds USA, Greenwich, CT). The signal was then amplified with AC (AM Systems, Carlsborg, WA) and DC (Brownlee Precision, Santa Clara, CA) amplifiers. Extracellular nerve stimulation was accomplished by placing the pair of wires used to record nerve activity into a stimulus isolation unit (Astromed/Grass Instruments, West Warwick, RI) that was connected to a S88 stimulator (Astromed/Grass Instruments).

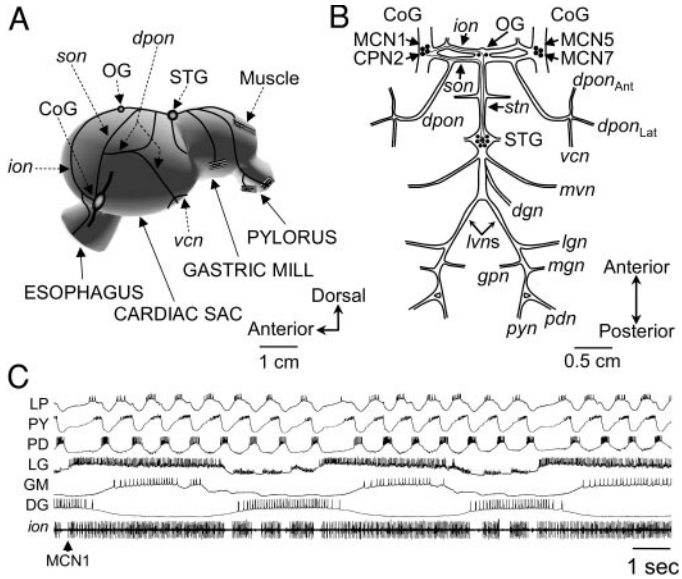

FIG. 1. Crab foregut and stomatogastric nervous system. *A*: schematic of crab foregut with innervating stomatogastric nervous system (STNS) in black. Arrows with full lines point to foregut regions. Arrows with dotted lines point to STNS elements. *B*: schematic of the isolated STNS. Included are the 4 ganglia, connecting nerves, peripheral nerves, and 4 identified CoG projection neurons. Each of these projection neurons occurs as a single copy in each CoG. *C*: motor patterns generated by the pyloric and gastric mill circuits in the STG. The *top* 3 intracellular recordings correspond to pyloric neurons and the *bottom* 3 intracellular recordings correspond to gastric mill neurons. Extracellular recording shows the activity of the MCN1 projection neuron. Abbreviations: Ganglia: CoG, commissural ganglion; OG, esophageal ganglion; STG, stomatogastric ganglion. Nerves: *dgn*, dorsal gastric nerve; *dpon*, dorsal posterior esophageal nerve; *gpn*, gastropyloric nerve; *ion*, inferior esophageal nerve; *lgn*, lateral gastric nerve; *lvn*, lateral ventricular nerve; *mgn*, medial gastric nerve; *mvn*, medial ventricular nerve; *pdn*, pyloric dilator nerve; *pyn*, pyloric nerve; *son*, superior esophageal nerve; *stn*, stomatogastric nerve; *vcn*, ventral cardiac nerve. Neurons: MCN1, 5, 7, modulatory commissural neuron 1, 5, 7; CPN2, commissural projection neuron 2; LP, lateral pyloric; PY, pyloric; PD, pyloric dilator; LG, lateral gastric; GM, gastric mill; DG, dorsal gastric.

Anatomy

VCN neurons were localized in the STNS with a methylene blue staining protocol (Alexandrowitcz 1951). Briefly, the STNS, includ-

ing the cardiac gutter, was dissected from the foregut. The preparation was then pinned out in a silicone elastomer-lined petri dish containing physiological saline. Next, the physiological saline was replaced with a methylene blue solution made with the following specifications: 100 ml cold physiological saline, 15 drops 1% aqueous methylene blue (Sigma), and 10 μL HCl (Sigma). The preparation was incubated in the methylene blue solution overnight at 4°C. The cardiac gutter was then examined for the presence of cell bodies with axons projecting through the *vcn*. Digital images were taken with the use of a Leica DMRB microscope and Leica DC 350FX digital camera system (Leica Microsystems, Bannockburn, IL). Images were acquired with Image-Pro Express software (Media Cybernetics, Silver Spring, MD).

Sensory stimulation

Semi-intact preparations containing the cardiac gutter were stimulated mechanically. In our semi-intact preparations, the section of stomach wall containing the cardiac gutter was connected to the STNS only by the *vcn/dpon*. The stimulus was delivered to the region of the cardiac gutter by gently applying pressure with a glass probe ending in a small (0.5 mm) blunt tip, roughly ¼ the size of the cardiac gutter. The probe was handcrafted by melting/pulling a Pasteur pipette and fire-polishing to remove any sharp edges that could cause tissue damage. In some experiments, the neighboring muscle (posterior inferior cardiac muscle, cv3) was transected to test the possibility that the VCN neurons were muscle stretch receptors.

Data analysis

Individual STNS neurons were identified by their axonal pathways, activity patterns, and interactions with other neurons (Blitz et al. 1999; Wood et al. 2000). Data were collected directly onto a MT-95000 chart recorder (Astromed, West Warwick, RI), and were simultaneously digitized (about 5 KHz) and collected onto a PC computer using data acquisition/analysis tools (Spike2, Cambridge Electronic Design, Cambridge, UK). Figures were made from Spike2 files incorporated into Adobe Photoshop (Adobe, San Jose, CA) and Powerpoint graphics programs (Microsoft, Seattle, WA). Statistical analyses were performed with SigmaStat 3.0 and SigmaPlot 8.0 (SPSS, Chicago, IL). Data are expressed as means ± SD.

Data analysis was facilitated with a custom-written program for Spike2 that determines the activity levels and phase relationships of neurons (freely available at http://www.neurobiologie.de/). Unless otherwise stated, each datum in a data set was derived by determining the average of 10 consecutive impulse bursts. Briefly, burst duration was defined as the duration (s) between the onset of the first and last action potential in an impulse burst. The firing rate of a neuron was defined as the number of action potentials minus 1, divided by the burst duration. The cycle frequency of pyloric and gastric mill rhythms was determined by calculating the inverse of the period between the onset of 2 successive pyloric dilator (PD) neuron bursts and 2 successive lateral gastric (LG) neuron bursts, respectively. The phase relationships among gastric mill neurons were determined relative to gastric mill cycles in which the onset and end of a cycle were designated by the onset of successive LG neuron bursts. Thus the phase onset and offset of each gastric mill neuron burst represented the fraction of a gastric mill cycle during which each neuron was active. Phase relationships were determined exclusively from extracellular recordings.

RESULTS

Anatomy and physiology reveal a population of peripheral VCN sensory neurons

The VCN neurons innervate a portion of the cardiac sac wall and project to the STNS through the ventral cardiac nerve (*vcn*) and the dorsal posterior esophageal nerve (*dpon*) (Fig. 2*A*). The *dpon* is a bilaterally symmetric nerve that branches from the superior esophageal nerve (*son*, Fig. 1, *A* and *B*). About 1 cm distal to the *son*, the *dpon* turns laterally and ventrally to project toward the ventral portion of the foregut. Near the ventral midline of the foregut, the *dpon* branches into 3 nerves (Figs. 1*B* and 2*A*). One branch ($dpon_{Ant}$) projects anteriorly, one branch ($dpon_{Lat}$) projects laterally, and one branch (*vcn*) projects posteriorly toward the posterior end of the cardiac sac compartment of the foregut (Fig. 2). Ringel (1924) described in detail the anatomical structures, including putative mech-

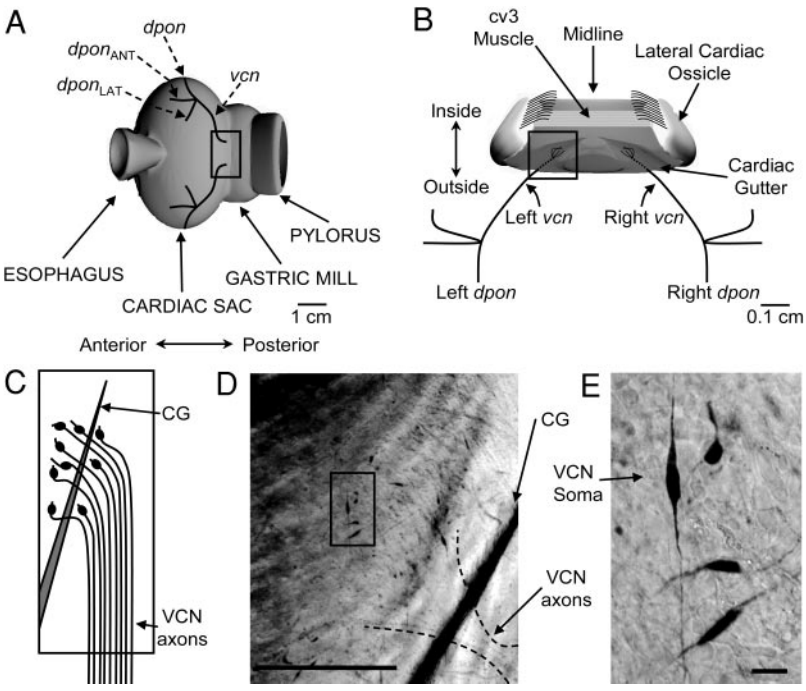

FIG. 2. Location and anatomy of VCN neurons. *A*: region of the foregut innervated by the *vcn* nerve. This schematic represents the ventral aspect of the foregut. *vcn* branches from the *dpon* and projects ventrally to innervate a region of the cardiac sac that lies on/near the ventral anteroposterior midline, near the gastric mill compartment (box). *B*: schematic representation of an enlarged view of the interior of the foregut region within the box of *A*. Here is located the cv3 muscle, between the paired lateral cardiac ossicles. *vcn* innervates (from the outside) the ipsilateral invagination (i.e., cardiac gutter) lying slightly anterior to the lateral cardiac ossicles. *C*: schematic of region found in the box of *B*. *D*: preparation consisting of the region found in the box of *B* stained with the vital dye methylene blue. One of 2 VCN axon bundles plus about 60 bipolar neurons (region within and near box) is shown. Dotted black lines indicate the location of exiting VCN axons. Cal. bar: 500 μm. *E*: higher-magnification view of region found in box of *D*, showing 4 VCN somata with proximal neurites. Cal. bar: 20 μm. CG: cardiac gutter.

anosensory neurons, found in this region of the crustacean foregut.

Several strategies were used to localize the VCN neurons in this region. First, we attempted to label the VCN neurons by placing the transected ends of either the *dpon* or *vcn* into small molecular weight dye for 24–48 h and allowing the dye to diffuse into the cut axons of the nerve (i.e., "nerve backfill"). In such experiments, the *vcn* remained attached to the cardiac sac wall (see Fig. 2*B*). Such backfilling techniques have been used successfully in the STNS to label the axons and somata of other neurons (Coleman et al. 1992). Nerve backfills ($n > 10$) using fluorescent dyes such as Lucifer yellow (10–20%) and rhodamine dextran (10–20%) were unsuccessful, partly because the portion of the stomach wall innervated by the *vcn* is autofluorescent (even when cleared with methylsalicylate). The autofluorescence made it impossible to visualize labeled axons projecting into the tissue. Backfills of the *vcn* using either of the nonfluorescent dyes nickel chloride (5%) or cobalt chloride (3%) ($n > 10$) also failed to yield labeling of any *vcn* axons projecting into the stomach wall. The VCN axon diameter at the point where the *vcn* enters the cardiac gutter was 1.2 ± 0.2 μm ($n = 5$). Therefore the lack of success with the backfills may have resulted from the small diameter of the *vcn* axons, perhaps because the small diameter axons did not remain open sufficiently long to enable much dye to diffuse into them. In fact, previous attempts to backfill several other STNS sensory neurons were also unsuccessful (Hooper et al. 1990; Sigvardt and Mulloney 1982).

We did successfully label the VCNs by staining the relevant region of the stomach wall with methylene blue, a neuronal stain used previously in the STNS (Dando and Maynard 1974; Wales et al. 1970). Methylene blue consistently stained a population of about 60 somata (range: 14–58; mean: 29.6 ± 18.4, $n = 5$) on each side of the midline region of the cardiac gutter innervated by the *vcn* (Fig. 2, *C* and *D*). The cardiac gutter is a bilaterally symmetrical invagination of the stomach wall near the cardiac sac–gastric mill boundary (see Fig. 2, *A* and *B*). Higher-magnification analysis revealed that these stained somata were bipolar (soma length: 24.7 ± 6.8 μm; soma width: 8.5 ± 1.6 μm, $n = 5$), with an apparently unbranched dendrite (about 60 μm long) and no evident associated specialization of the surrounding tissue (Fig. 2*E*). One process of each cell projected through the *vcn*, whereas the presumed dendrite of the cell appeared to be imbedded within the stomach wall. These somata were not visible in unstained preparations and attempts to find them for intracellular recording were unsuccessful.

We used *vcn* stimulation to gain further evidence that the VCN system corresponds to a population of neurons, rather than a single sensory neuron. To this end, we used an identified motor neuron of the esophageal motor system [esophageal motor neuron (OMN)] as an assay for VCN neuron action. The OMN occurs as a single copy in each CoG and has the largest amplitude spontaneously active action potential in extracellular *ion* recordings (data not shown). Its soma (diameter about 50 μm) is located near those of modulatory commissural neuron 1 (MCN1) and MCN5 (see Coleman and Nusbaum 1994; Norris et al. 1996). Stimulating the *vcn* evoked a constant-latency excitatory postsynaptic potential (EPSP) in the ipsilateral OMN. This PSP persisted in the presence of high-divalent cation saline ($n = 6$) (Fig. 3), indicating that the influence of

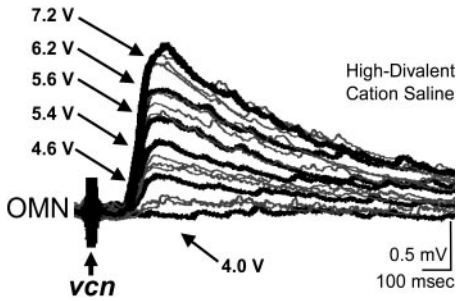

FIG. 3. Physiological evidence for a population of VCN neurons. Shown is an intracellular recording of an esophageal system motor neuron (OMN) located in the CoG. Single *vcn* nerve stimuli at voltages sufficient to activate the VCN pathway elicited apparently monosynaptic excitatory postsynaptic potentials (EPSPs) in the OMN. As the stimulus voltage was increased from threshold (4.2 V) to maximal response (7.2 V) in 0.2-V increments, the EPSP amplitude increased with no change in latency and no additional peaks evident. Shown are all 17 averaged EPSPs (black and gray) evoked by *vcn* stimulation. Representative EPSPs demonstrating that EPSP amplitude increases with increased *vcn* stimulation voltage are shown in thick black. This result indicates that more presynaptic neurons of the type responsible for the low-amplitude stimulus-evoked EPSP were likely being recruited. Each EPSP is the average of 10–12 individual responses.

the VCN neurons on the OMN is likely to be monosynaptic. Gradually increasing the *vcn* stimulus strength resulted in several stepwise increases in the amplitude of the PSP evoked in the OMN ($n = 6$) (Fig. 3). One plausible explanation for this effect is that with each step increase in the *vcn* stimulus voltage, an additional subset of VCN axons was activated, resulting in the recorded increase in PSP amplitude in the OMN. However, an alternate hypothesis is that each increase in PSP amplitude reflects the addition of a single VCN neuron and that a relatively small number of VCN neurons were recruited by *vcn* stimulation (e.g., 12 VCN neurons in Fig. 3).

Area containing the VCN somata is sensitive to mechanical stimulation

To determine the nature of the stimulus required to activate the VCN neurons, we subjected the relevant region of stomach wall to different types of sensory stimuli. First, we tested the hypothesis that the VCN neurons are chemoreceptors by determining whether exposing the relevant stomach region to 2 diet staples, macerated clams and squid, had any effect on the STNS. Similar food extracts were successfully used to activate esophageal chemoreceptors in the lobster (Robertson and Laverack 1979). When introduced to the cardiac gutter, however, no effect on either the pyloric or the gastric mill rhythm was ever observed ($n = 5$). Next, we tested the hypothesis that the VCN neurons are proprioceptive because intrinsic muscles occur in the region where the VCN somata are located. However, artificially stretching these muscles with a glass probe had no effect ($n = 6$). Furthermore, evoking muscle contractions by activating the motor neuron (IC neuron) innervating these muscles also had no effect ($n = 2$). Moreover, as discussed in the following text, transecting these muscles did not alter the mechanoreceptive function of the VCNs. Finally, we examined whether gently pressing portions of the relevant stomach region with a blunt glass probe (diameter = 0.5 mm) elicited a response. This stimulus did reliably evoke STNS responses when gentle pressure was exerted on a specific area of the stomach wall, that is, the cardiac gutter ($n > 15$).

Specifically, during single, brief (3–5 s) applications of pressure, the pyloric rhythm consistently responded with an increased cycle frequency for the duration that pressure was applied. In response to repetitive probing, a long-lasting gastric mill rhythm was activated. These effects are explored below.

We also tested the hypothesis that the VCN neurons receive a chemical synapse in the stomach lining from a primary transducing element. To this end, we placed the patch containing the VCN neurons in a Vaseline well and replaced the normal saline in the well with low Ca^{2+} (0.1× normal/added Mn^{2+}) saline to block transmitter release. In 3 out of 3 experiments, pressure applied to the cardiac gutter when bathed in low Ca^{2+} saline still excited the pyloric rhythm and activated the gastric mill rhythm.

Physiological activity patterns of VCN neurons

We sought to characterize the response of the VCN neurons to pressure applied to the cardiac gutter. However, we failed to record VCN activity either intracellularly or extracellularly. As indicated above, we were unable to localize the VCN somata in physiological preparations, making intracellular recordings impractical. Furthermore, we were not able to record extracellular VCN activity in either the *vcn* or the *dpon* in response to pressure applied to the cardiac gutter. Similarly, no time-locked events were recorded in the *dpon* in response to extracellular *vcn* stimulation (0/10), despite this stimulus having actions within the STNS. Averaging the responses of many (50–150) individual *vcn* stimulations also failed to unmask the VCN action potential, despite recording the desheathed *dpon* nerve where axonal activity is not muted by the presence of a connective tissue sheath surrounding the nerve ($n = 4$). Because the amplitude of an extracellularly recorded action potential is related to the axon diameter of the active neuron, we hypothesize that the relatively small axon diameter of the VCN neurons produces action potentials that are lost in the noise of the extracellular recording.

VCN alteration of the pyloric rhythm

Briefly (2–5 s) applying pressure to the cardiac gutter with a glass probe had several effects on the pyloric rhythm (Fig. 4). The most dramatic effects included an increase in the cycle frequency of the pyloric rhythm and decrease in lateral pyloric (LP) neuron activity. The pyloric cycle frequency increased from 1.17 ± 0.11 Hz before stimulation to 1.30 ± 0.13 Hz during stimulation (11% increase, $P < 0.05$, $n = 6$), and returned to 1.23 ± 0.09 Hz during the first 5 cycles after stimulation. LP neuron activity, as determined by the number of action potentials it fired per impulse burst, decreased from 5.2 ± 2.3 spikes/burst before stimulation to 2.9 ± 2.2 spikes/burst during stimulation (45% decrease, $P < 0.05$, $n = 6$), and increased back to 4.2 ± 1.9 spikes/burst after stimulation. These actions on the pyloric neurons were strongest during the application of pressure and waned within a few seconds after the application (Fig. 4).

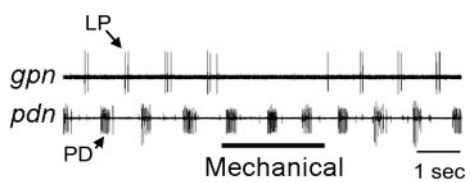

FIG. 4. Mechanical stimulation of the cardiac gutter modulates an ongoing pyloric rhythm. Slight pressure to the cardiac gutter (see Fig. 2), on an excised portion of the cardiac sac innervated by the *vcn* (see Fig. 2) still connected to the isolated STNS, inhibited the LP neuron and increased the frequency of occurrence of PD neuron bursts (pyloric cycle frequency).

To better control the delivery of the sensory stimulus, we determined whether extracellular stimulation of the nerves connecting the cardiac gutter with the STNS (i.e., *vcn* and *dpon*; see Figs. 1 and 2) was sufficient to mimic the mechanically evoked actions on the pyloric neurons. Indeed, short-duration (2–5 s) suprathreshold tonic stimulation (15 Hz) of either the *vcn* or *dpon* elicited a pyloric response that was comparable to that elicited by pressure application to the cardiac gutter (Fig. 5*A*). In all 3 cases (*dpon*, *vcn*, or mechanical stimulation), the stimulus significantly increased the pyloric cycle frequency and decreased LP neuron activity (Fig. 5, *B* and *C*). Furthermore, these actions followed similar time courses (Fig. 5, *B* and *C*). The 3 stimulation modes also significantly decreased LP neuron burst duration (Fig. 5*D*) but failed to change PD neuron burst duration (Fig. 5*E*). In general, however, *dpon* and *vcn* nerve stimulation consistently yielded stronger responses than mechanical stimulation. This difference was presumably attributable to the ability to more faithfully activate a larger population of VCN neurons with nerve stimulation than mechanical stimulation. Furthermore, although nerve stimulation faithfully elicited these effects at lower stimulation frequencies (e.g., 5 Hz), more robust actions on the pyloric rhythm were observed with higher frequencies (e.g., 15 Hz). Finally, stimulation of the 2 remaining *dpon* branches, the $dpon_{Lat}$ (lateral branch of the *dpon*) and the $dpon_{Ant}$ (anterior branch of the *dpon*), failed to produce any actions on the pyloric and gastric mill neurons ($n = 5$, data not shown).

VCN activation of the gastric mill rhythm

Whereas single applications of pressure to the cardiac gutter influenced the pyloric rhythm, multiple pressure applications in succession also activated the gastric mill rhythm. Using a glass probe, we applied rhythmic pressure to the cardiac gutter, delivering between 5 and 10 stimuli at a rate of one stimulus (duration: 3–4 s) per 10–15 s. During the delivery of such stimuli, uncoordinated bursting in gastric mill neurons was observed. Within 10–20 s *after* the delivery of the last in a succession of pressure applications, the bursting among gastric mill neurons became more regular and coordinated and a long-lasting gastric mill rhythm commenced (Figs. 6 and 7*A*, $n > 15$). The gastric mill rhythm elicited with 10 rhythmic presses was often strongest during the first 5 min after the rhythmic stimulation, and would gradually wane until the rhythm would terminate. This rhythm persisted for as long as 30 min, with its termination occurring on average 14 min after stimulation (Fig. 7*B*).

We fully characterized the resulting gastric mill rhythm 1 min after rhythmic pressure applications to the cardiac gutter, including determining the activity of gastric mill motor neurons (Table 1, Fig. 7). At this time, the cycle period of the gastric mill rhythm was 10.9 ± 2.6 s ($n = 6$) (Table 1, Fig. 7*C*). The duration of the impulse burst for neurons involved in the mechanically evoked gastric mill rhythm is presented in

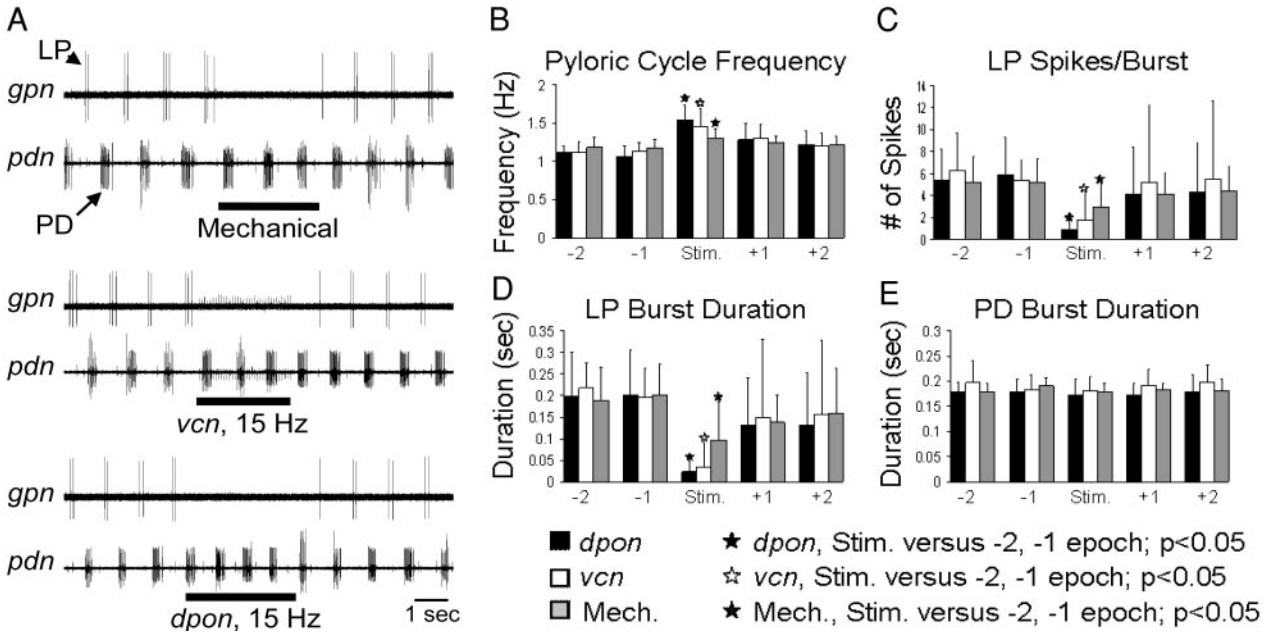

FIG. 5. Effects of brief mechanical stimulation of the ventral cardiac gutter are mimicked by either *vcn* or *dpon* nerve stimulation. *A*: effects of mechanical, *vcn*, and *dpon* stimulation in the same preparation. In each case, the stimulus inhibited LP neuron activity and increased the frequency of the pyloric rhythm (as measured by PD neuron burst frequency). *B–E*: quantification of the pyloric rhythm in response to mechanical, *vcn*, or *dpon* stimulation. Data represented come from 6 preparations in which all 3 modes of stimulation were delivered. Events occurring during VCN stimulation are labeled "Stim." Bars labeled "−2" and "−1" correspond to 2 consecutive epochs immediately before VCN stimulation, and those labeled "+1" and "+2" correspond to 2 consecutive epochs immediately after stimulation. Data in each epoch represents the average of 5 consecutive pyloric cycles. Pyloric cycle frequency, number of LP spikes/burst, and LP burst duration are significantly different during the stimulus vs. prestimulus epochs ($n = 6$, $P < 0.05$, one-way repeated-measures ANOVA, Student–Newman–Keuls method).

Table 1 and Fig. 7*D*. The activity of all analyzed neurons was relatively high. For example, the LG neuron fired on average 67 action potentials per burst, the DG neuron fired 47 action potentials per burst, and the AM neuron fired 36 action potentials per burst (Table 1, Fig. 7, *E* and *F*).

In general, the impulse bursts of the LG and GM neurons alternated with those of the DG, AM, IC, and VD neurons (Table 1, Figs. 6 and 7*G*). To quantify these temporal relationships we expressed the bursting of the neurons involved in the gastric mill rhythm with respect to a normalized cycle period, where the start of an LG neuron impulse burst marked the start of the cycle and the start of the next LG impulse burst marked the end of the cycle. Thus the LG and GM neuron impulse bursts occurred during the first half of each cycle, whereas the DG and AM neuron bursts started in the latter half of the cycle and terminated during the beginning of the subsequent cycle (Table 1, Fig. 7*G*). The IC and VD neurons collectively burst during the latter two thirds of the cycle ($n = 3$) (Table 1, Fig. 7*G*).

Rhythmically stimulating either the *dpon* or the *vcn* routinely activated a gastric mill rhythm that was indistinguishable from the mechanically evoked rhythm on nearly all tested parameters. Thus stimulating either nerve (rhythmic stimulus train: 10 × 6 s burst delivered at 0.06 Hz; 15 Hz intraburst stimulation rate) produced a long-lasting (*dpon*: 1043 ± 947.5 s, $n = 6$; *vcn*: 1131.7 ± 902.9 s, $n = 6$) gastric mill rhythm in which the impulse bursts of all involved neurons had burst durations, activity levels, burst onsets, and burst offsets that were identical to those derived from the mechanical stimulus except DG firing frequency (Table 1, Fig. 7). Furthermore, the evolution of the gastric mill rhythm was reminiscent of those evoked mechanically in that regular, coordinated gastric mill

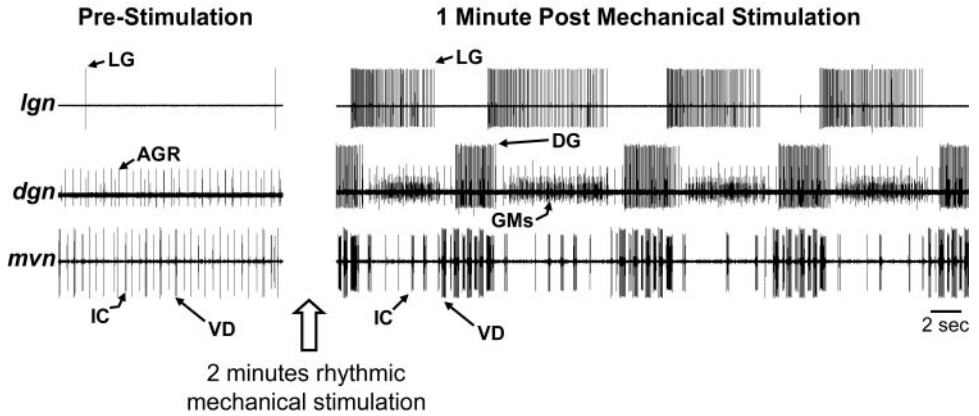

FIG. 6. Repetitive mechanical stimulation of the ventral cardiac gutter activates the gastric mill rhythm. *Left*: before stimulation, there was no gastric mill rhythm (*lgn, dgn, mvn*) but there was a pyloric rhythm (*mvn*). Anterior gastric receptor (AGR) neuron is a Golgi tendon organlike sensory neuron that fires tonically in the isolated STNS (Combes et al. 1995). *Right*: rhythmic applications of pressure to the cardiac gutter (see Fig. 2), in an excised portion of the cardiac sac innervated by the *vcn* (see Fig. 2) still connected to the isolated STNS, activated the gastric mill rhythm.

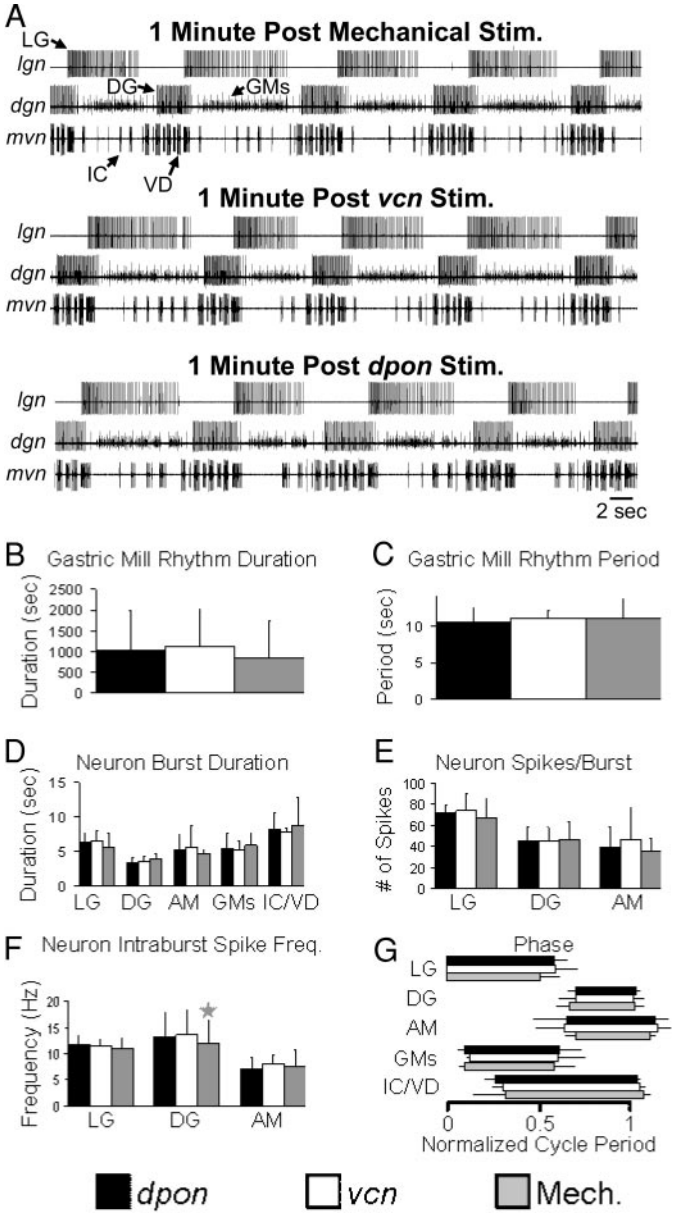

FIG. 7. Effects of repetitive mechanical stimulation are mimicked by either repetitive *vcn* or *dpon* nerve stimulation. *A*: gastric mill rhythms elicited by repetitive mechanical, *vcn*, or *dpon* stimulation in the same preparation. In each case, the stimulus activated rhythmic bursting in the LG ($n = 6$), DG ($n = 6$), and GM ($n = 4$) neurons, as well as gastric mill rhythm-timed inhibition of the IC and VD neurons ($n = 3$). *B–G*: quantification of several gastric mill rhythm parameters in response to mechanical, *vcn*, or *dpon* stimulation. Regardless of the stimulus, the characteristics of the resulting motor pattern were similar ($P > 0.05$, one-way repeated-measures ANOVA), except for DG neuron firing frequency ($P < 0.05$).

neuron bursting activity commenced within 10–20 s after the stimulus train. This finding provided us the confidence to proceed with the characterization of this sensory pathway using more detailed intracellular analyses that were afforded by nerve stimulation protocols.

Different dpon nerve stimulation protocols evoke similar gastric mill rhythms

Without the ability to record VCN activity, we were unable to characterize the response of the VCN neurons to mechanical stimulation. Therefore we could not apply the behaviorally relevant stimulation pattern to the *vcn* or *dpon*. To circumvent this problem, we examined the response of the gastric mill circuit to 3 different *dpon* nerve stimulation protocols. Because the VCN neurons are sensitive to mechanical movements, we activated the VCN neurons with stimulus patterns that mimic the possible biomechanical movements these neurons may encounter. These include foregut movements produced in response to motor patterns generated by the STNS (e.g., pyloric, gastric mill, and cardiac sac rhythms), and pressure on the stomach wall produced by the constant presence of stored food (e.g., tonic activity). Thus we stimulated the *dpon* in rhythmic patterns reminiscent of either a slow gastric mill rhythm and fast cardiac sac motor pattern ("gastric mill/cardiac sac" stimulation protocol) or a pyloric rhythm ("pyloric" stimulation protocol), or stimulated the *dpon* tonically ("tonic" stimulation protocol). From these experiments, the parameter most influential for the activation and maintenance of a robust gastric mill rhythm was the absolute duration of stimulation. Short-duration stimulation protocols, such as those that selectively influenced the pyloric rhythm (see Fig. 5), were not sufficient to elicit the gastric mill rhythm, regardless of the stimulation pattern. Generally, only stimulations in excess of about 1 min activated robust, long-lasting gastric mill rhythms (data not shown). Furthermore, during these longer-duration stimulus protocols, when the stimulus frequency was decreased below 5 Hz the resulting gastric mill rhythm became less robust (data not shown). Thus we compared different stimulation protocols (i.e., gastric mill/cardiac sac, pyloric, and tonic) with stimulus frequencies in the moderate range (15 Hz). With respect to the parameters analyzed (i.e., gastric mill cycle period and LG neuron duty cycle), the rhythms produced by long-duration rhythmic (either gastric mill/cardiac sac or pyloric protocol) and tonic *dpon* stimulation were the same (Fig. 8). This conclusion was also supported by a qualitative assessment of the other aspects of these rhythms. Thus although we cannot be sure that we are reproducing the physiological response profile of the VCN neurons when we stimulate the *vcn* or *dpon* nerves, we are confident that the gastric mill rhythm produced by our stimulation protocols is likely to be a close approximation to the rhythm produced under normal behavioral conditions.

VCN activation of the gastric mill rhythm requires projection neuron activation in the commissural ganglia

The production of the gastric mill rhythm requires the activation of particular projection neurons in the commissural ganglia (CoGs; see Fig. 1) that are normally not spontaneously active in *C. borealis* (Nusbaum and Beenhakker 2002; Nusbaum et al. 2001). Therefore we predicted that the VCN neurons would not activate the gastric mill rhythm after the CoGs were removed from the STNS. To test this hypothesis, we transected the *ion*s and *son*s. We transected each *son* between the CoG and *dpon*, thereby enabling the VCN neurons to still have potential access to the STG by the *son* and *stn* (see Fig. 1). When the CoGs were removed, stimulating the VCN neurons, either mechanically ($n > 10$) or by stimulating the

TABLE 1. *Parameters of gastric mill rhythm resulting from mechanical, vcn, or dpon stimulation*

	Mechanical	*vcn*	*dpon*	*P*
		Burst duration (s)		
LG	5.7 ± 1.9	6.5 ± 1.5	6.3 ± 1.3	0.64
DG	3.9 ± 0.8	3.5 ± 0.8	3.5 ± 0.6	0.43
AM	4.7 ± 0.6	5.6 ± 3.2	5.4 ± 2.2	0.85
GMs	6.0 ± 1.6	5.4 ± 1.2	5.5 ± 2.1	0.79
IC/VD	8.8 ± 4.0	7.9 ± 0.5	8.2 ± 2.4	0.83
		Spikes/burst		
LG	67.3 ± 18.0	73.6 ± 16.0	71.3 ± 8.4	1.00
DG	46.8 ± 17.0	45.5 ± 12.8	45.7 ± 12.1	0.94
AM	35.5 ± 11.8	46.4 ± 29.7	39.1 ± 19.4	0.62
		Firing frequency (Hz)		
LG	11.0 ± 1.8	11.5 ± 1.2	11.8 ± 1.6	0.73
DG	11.9 ± 4.6	13.6 ± 4.8	13.3 ± 4.5	0.04
AM	7.6 ± 3.2	7.9 ± 1.7	7.0 ± 2.3	0.43
		Period (s)		
	11.0 ± 2.6	10.9 ± 1.1	10.5 ± 1.7	0.14
		Rhythm duration (s)		
	846.7 ± 893.7	1131.7 ± 902.9	1043.7 ± 947.6	0.90
		Phase (% of gastric mill rhythm cycle)		
		ON		
LG	0	0	0	1.00
DG	67.5 ± 7.3	70.4 ± 9.1	70.7 ± 4.2	0.28
AM	71.2 ± 6.2	64.6 ± 16.0	65.8 ± 18.4	0.55
GMs	9.7 ± 3.0	12.4 ± 1.0	9.8 ± 3.3	0.32
IC/VD	31.8 ± 17.6	30.9 ± 5.6	26.5 ± 5.9	0.74
		OFF		
LG	51.4 ± 10.3	59.4 ± 12.8	58.6 ± 7.5	0.12
DG	103.5 ± 4.4	102.4 ± 5.5	103.6 ± 2.0	0.77
AM	111.2 ± 3.0	115.7 ± 7.3	114.4 ± 6.8	0.57
GMs	58.8 ± 11.3	61.0 ± 14.8	61.8 ± 12.0	0.74
IC/VD	108.3 ± 3.6	105.9 ± 2.8	104.7 ± 1.4	0.06

Data for these rhythms come from preparations in which the gastric mill rhythms resulting from all modes of stimulation were analyzed. Thus parameters were tested with one-way repeated-measures ANOVAs. Normality tests failed for LG Spikes/burst and LG Phase ON, and thus repeated-measures ANOVAs on ranks were performed. Period, $n = 6$; Duration, $n = 6$; LG, $n = 6$; DG, $n = 6$; AM, $n = 3$; GMs, $n = 4$; IC/VD, $n = 3$.

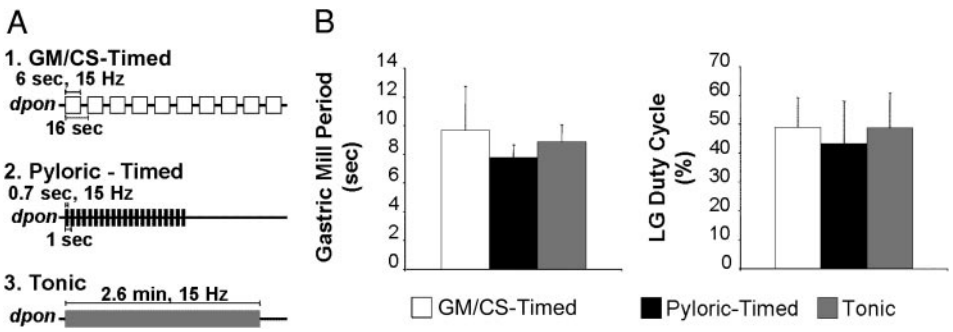

FIG. 8. Different *dpon* nerve stimulus patterns have the same influence on the gastric mill rhythm. *A*: types of stimulus protocols used to activate VCN pathway. Using the *dpon*, the VCN pathway was stimulated with a protocol reminiscent of either the gastric mill/cardiac sac (GM/CS) or pyloric rhythm, or was stimulated tonically. In each case, 900 individual stimuli were delivered. *B*: resulting gastric mill rhythm was assessed 1 min after each stimulation. Based on the 2 parameters tested, gastric mill cycle period ($n = 5$, $P = 0.42$) and LG neuron duty cycle ($n = 5$, $P = 0.74$), the gastric mill rhythms generated by the 3 protocols outlined in *a* are comparable (one-way ANOVA).

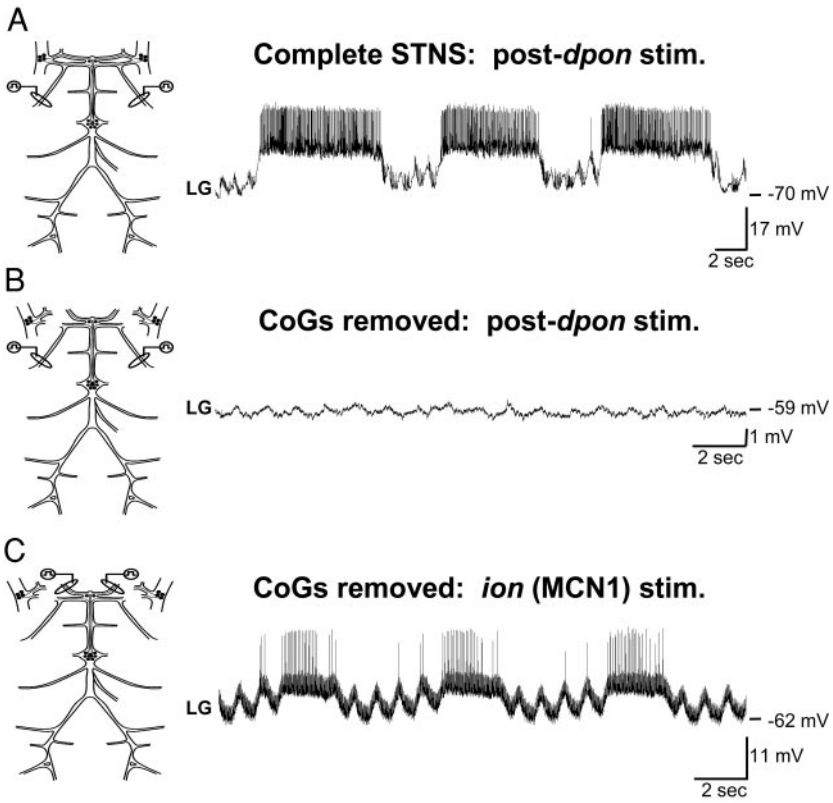

FIG. 9. Activation of the gastric mill rhythm by VCN stimulation requires communication between the commissural ganglia (CoGs) and the STG. *A*: in the complete STNS, activating the VCN pathway by *dpon* stimulation initiated the gastric mill rhythm. *B*: after removing the CoGs from the STNS, stimulating the VCNs no longer activated the gastric mill rhythm. *C*: after removing the CoGs, tonic extracellular stimulation (25 Hz) of MCN1 (*ion*, see Fig. 1) still activated the gastric mill rhythm, indicating that the gastric mill circuit was not compromised. Thickened baseline results from tonic barrage of EPSPs from MCN1 (Coleman et al. 1995). All 3 panels are from the same STNS.

dpon/*vcn* nerves ($n > 10$), never elicited a gastric mill rhythm from the STG (Fig. 9). Nonetheless, activating modulatory commissural neuron 1 (MCN1; see following text) in these same preparations by extracellular *ion* stimulation activated a gastric mill rhythm, indicating that the gastric mill circuit was not compromised by removing the CoGs (Fig. 9*C*). We therefore determined which identified CoG projection neurons were activated by VCN stimulation and so might contribute to activation of the gastric mill rhythm in the STG.

Four of the approximately 20 CoG projection neurons that influence the STG are identified and at least partially characterized. These include MCN1, MCN5, MCN7, and commissural projection neuron 2 (CPN2) (Blitz et al. 1999; Norris et al. 1994, 1996; Wood and Nusbaum 2002). MCN1 and MCN5 activity is readily recorded extracellularly in the *ion* (Coleman and Nusbaum 1994; Norris et al. 1996), which enabled us to determine directly that they were activated by mechanically activating the VCN neurons ($n = 6$). MCN5 was consistently activated quickly, whereas repeated probes gradually activated MCN1 ($n = 6$). We used an indirect monitor to determine whether CPN2 was also activated by mechanical activation of this sensory pathway. Specifically, CPN2 appears to be the only projection neuron that activates the gastric mill GM neurons (Norris et al. 1994). Thus because the GM neurons actively participate in the mechanically activated gastric mill rhythm (see Fig. 7), it appeared likely that CPN2 was also activated by such stimulation.

Activating the VCN pathway by *vcn* or *dpon* stimulation influenced all 4 of the CoG projection neurons in ways that were comparable to mechanical stimulation. Specifically, MCN5 was excited *during dpon* stimulation (firing frequency: 16.2 ± 1.7 Hz, $n = 5$) but its activity waned within seconds (14.5 ± 2.0 s, $n = 5$) *after* stimulation and remained tonically active at a slower firing frequency (3.0 ± 1.4 Hz, $n = 5$) for 1–2 min. Previous work demonstrated that MCN5 must be firing in excess of 20 Hz to strongly influence the STG circuits (Norris et al. 1996). MCN1 ($n > 10$) and CPN2 ($n = 8$) were initially inhibited *during* VCN stimulation but exhibited strong activity for tens of minutes *after* VCN stimulation (Fig. 10). The MCN7 response to VCN stimulation was similar to the MCN1/CPN2 response but much weaker ($n = 4$) (Fig. 10). In some preparations, the inhibition of MCN1/CPN2 exhibited during VCN stimulation was overcome by the longer-lasting excitation provided by this pathway and, consequently, these projection neurons occasionally became active toward the end of the stimulus delivery (see Fig. 10).

Single *dpon* stimuli consistently evoked postsynaptic responses in CoG neurons, including EPSPs in the OMN ($n = 5$) and MCN5 ($n = 7$), and complex postsynaptic potentials (PSPs) in MCN1 ($n = 8$), MCN7 ($n = 4$), and CPN2 ($n = 3$). The complex PSP consisted of a relatively long-duration (about 80 ms) EPSP interrupted by a shorter-duration (about 40 ms) inhibitory PSP (Fig. 11). Furthermore, the postsynaptic events in these neurons included an additional long-duration (about 2 s) depolarization, suggesting a modulatory action. A portion of these postsynaptic events persisted in high-divalent cation saline (Fig. 11), indicating that these events were likely to result directly from the action of the VCN neurons. Specifically, the EPSP in MCN1 ($n = 5$), MCN7 ($n = 2$), and CPN2 ($n = 2$), but not in MCN5 ($n = 2$), persisted in the high-divalent cation saline. The longer-duration actions on MCN1, MCN7, and CPN2 also appeared to be monosynaptic. In contrast, the IPSP in MCN1, MCN7, and CPN2 did not persist in the high-divalent cation saline (Fig. 11, *bottom*), supporting the

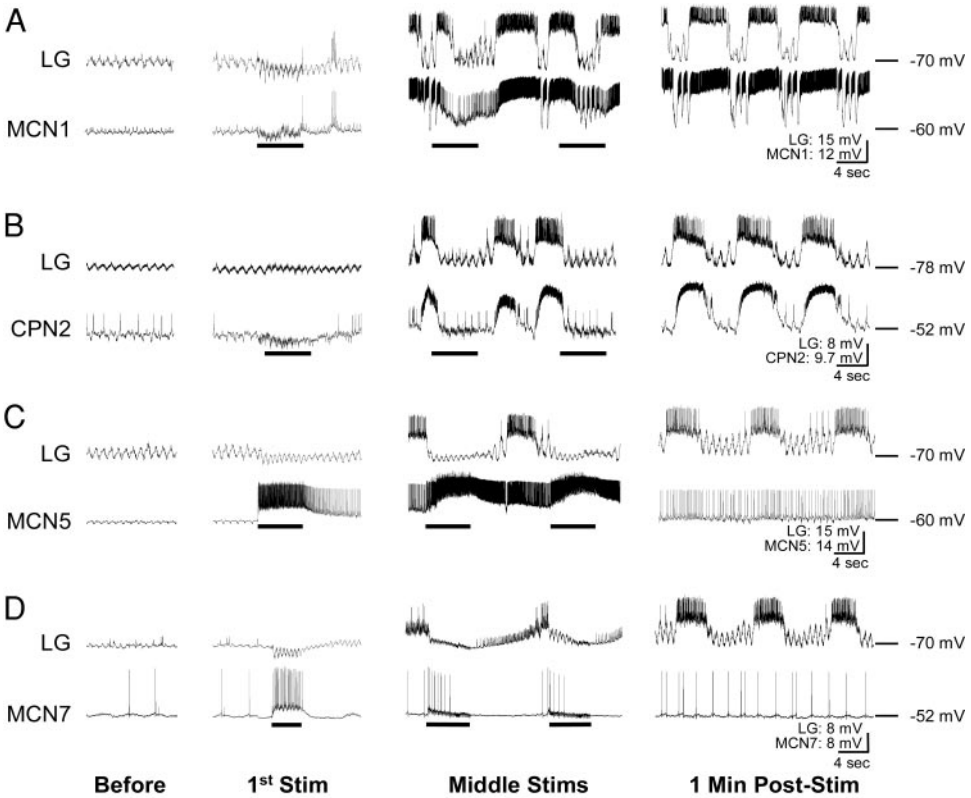

FIG. 10. Extracellular *dpon* stimulation influences CoG projection neurons. Shown are intracellular recordings of each identified CoG projection neuron in response to a train of 10 *dpon* stimuli (train frequency: 0.06 Hz; stimulus duration: 6 s; stimulus frequency: 15 Hz). *A*: MCN1. Initially, stimulating the *dpon* caused MCN1 to hyperpolarize slightly, followed by a mild rebound after stimulation (*1st Stim*). During the course of the train delivery, VCN excitation of MCN1 built up until MCN1 exhibited strong activity. Nonetheless, MCN1 continued to hyperpolarize in response to *dpon* stimulation (*Middle Stims*). MCN1 exhibited strong activity 1 min after the *dpon* train. *B*: CPN2. Response of CPN2 to a *dpon* stimulus train was similar to that of MCN1. Initial CPN2 inhibition was gradually overcome by strong excitation. After the *dpon* train, CPN2 was highly active. *C*: MCN5. MCN5 was activated by *dpon* stimulation. This level of activation built up during the course of the *dpon* train. After the stimulus train, MCN5 was weakly or not active. *D*: MCN7. MCN7 is only weakly excited by a *dpon* stimulus. After the delivery of *dpon* train, MCN7 was weakly or not active.

presence of a polysynaptic pathway for the inhibitory component.

VCN neurons have cholinergic actions on projection neurons

In an effort to understand which neurotransmitter(s) underlie these EPSPs, we used pharmacological agents that block the actions of various neurotransmitters. We examined whether the VCN neurons were serotonergic, given that one set of identified STNS muscle stretch receptor neurons use serotonin as a cotransmitter (Katz and Harris-Warrick 1990). However, 2 antagonists that block serotonergic actions in the crustacean STNS, atropine (10^{-4} M) and cinanserin (10^{-4} M), did not suppress the *dpon*-evoked EPSPs in the OMN and MCN1 ($n > 3$, data not shown). Because many mechanoreceptors in arthropods use acetylcholine as a neurotransmitter (Katz et al. 1989; Miller et al. 1992), we investigated whether the VCN neurons used this transmitter to influence the OMN and MCN1. The direct EPSPs in the OMN and MCN1 were indeed partially suppressed by the nicotinic acetylcholine receptor antagonist, decamethonium bromide (10^{-3} M). This antagonist, superfused in high-divalent cation saline, reversibly reduced the amplitude of the *dpon*-evoked EPSPs in these neurons by about 40% ($n = 3$) (Fig. 12). Additionally, we attempted to block the long-lasting component of the EPSPs in the OMN and MCN1 using the muscarinic cholinergic antagonists scopolamine (10^{-4} M) and atropine (10^{-3} M). These antagonists were previously used in the STNS to block muscarinic actions (Katz and Harris-Warrick 1989; Marder and Paupardin-

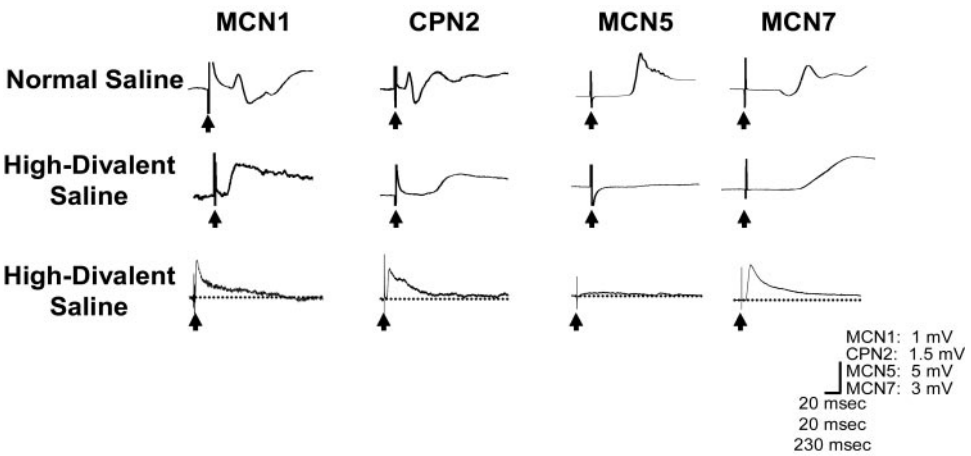

FIG. 11. Synaptic actions on CoG projection neurons resulting from *dpon* stimulation. In normal saline, MCN1, CPN2, and MCN7 received complex PSPs from *dpon* stimulation. This PSP consisted of a relatively long-duration EPSP interrupted by a shorter-duration IPSP. Only the EPSP persisted in the presence of high-divalent cation saline in MCN1, CPN2, and MCN7, suggesting a monosynaptic action. Furthermore, this presumed monosynaptic component included a long-lasting action (*bottom traces*). Stimulating the *dpon* also elicited an EPSP in MCN5. This postsynaptic event did not persist in high-divalent cation saline. Each PSP is the average of 10 individual postsynaptic responses. Arrows indicate stimulus artifact. Vm_{Rest}: MCN1, −67 mV; CPN2, −57 mV; MCN5, −62 mV; MCN7, −72 mV.

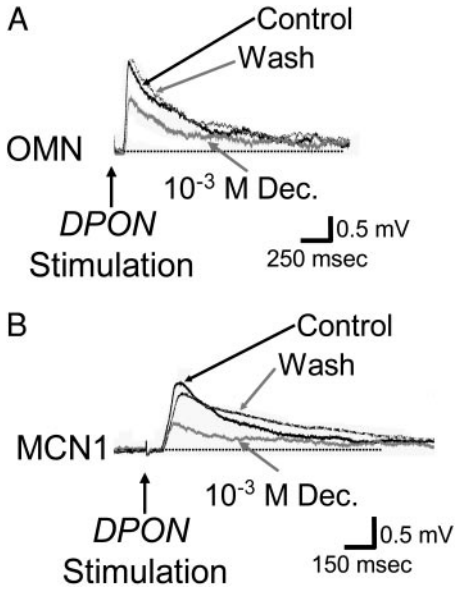

FIG. 12. VCN neurons are cholinergic. *A*, *B*: intracellular recordings of CoG neurons (OMN and MCN1) in high-divalent cation saline while single stimuli were delivered to the *dpon* revealed presumably monosynaptic EPSPs. Amplitude of these EPSPs was reversibly reduced by about 40% when the cholinergic antagonist decamethonium bromide (10^{-3} M) was superfused. Each PSP is the average of about 30 postsynaptic events. Vm_{Rest}: OMN: −54 mV; MCN1, −75 mV.

Tritsch 1978). However, neither antagonist attenuated the VCN-evoked response in either the OMN or MCN1 ($n = 3$).

DISCUSSION

In this study we have described features of a newly identified sensory system in the stomatogastric nervous system of *C. borealis*. This system includes a population of small bipolar neurons that innervate the wall of the cardiac gutter of the crab foregut. The cardiac gutter is located near the junction of the cardiac sac and gastric mill compartments of the foregut, and is innervated by a branch (*vcn*) of the *dpon*. Thus we have called these neurons the ventral cardiac neurons (VCNs). We postulate that these neurons are equivalent to the neurons Ringel (1924) initially identified anatomically in this region of the crayfish, *Astacus fluviatilis*, and Dando and Maynard (1974) later identified anatomically in crab (*Callinectes sapidus*) and lobster (*Panuliris argus*). These neurons do not appear to have chemoreceptive properties. Rather, they are activated by pressure applied to the cardiac gutter. When activated for short durations (5–10 s), the VCNs modulated the pyloric rhythm, and when activated for longer durations (>1 min) they evoked a long-lasting activation of CoG projection neurons that in turn elicited a long-lasting activation of the gastric mill rhythm. Here, we have focused primarily on these latter actions.

Behavioral model for VCN neurons

Because of a limited understanding of the biomechanical underpinnings of the foregut during food processing, we can only speculate as to the behavioral function of the VCN neurons. However, based on findings described in other sensory systems, we hypothesize that the VCNs sense movements within the foregut. Functionally analogous sensory neurons have been described in the foregut of insects (Gelperin 1967; Orlov 1924, 1925; Rice 1970). For example, the proper coordination of foregut movements produced by the stomatogastric nervous system of the European house cricket, *Acheta domesticus*, is thought to involve the interaction between a population of foregut body wall mechanoreceptors and esophageal motor neurons (Mohl 1972). Functionally similar stomach-distention receptors in the blood-feeding insect, *Rhodnius prolixus* (Bennet-Clark 1966; Chiang and Davey 1988; Chiang et al. 1990) are thought to initiate endocrinological processes underlying molting and egg production (Chiang and Davey 1988). Compartment distention-sensitive mechanoreceptor neurons also innervate the cricket (*Teleogryllus commodus*) genital chamber, a compartment transiently housing the egg during oviposition behavior (Sugawara and Loher 1986). These neurons sense the distention of the genital chamber produced by the egg in the ovipositing female and are responsible for the rest phase in the egg-laying behavior (Sugawara 1993, 1996).

In line with these previous studies, our current hypothesis regarding the VCN neurons is that they function as mechanoreceptor neurons that are activated during stomach distention resulting from food intake, thereby providing a trigger for the activation of food chewing when the food is subsequently moved to the gastric mill compartment (Fig. 13). Our finding that the gastric mill circuit is primarily activated for long durations *after* VCN stimulation supports this hypothesis. Rigorously testing this hypothesis, however, will require both a more detailed anatomical description of the VCN neurons and a detailed characterization of how food intake influences the morphology of the crab foregut.

Long-lasting nature of VCN actions

Relatively brief VCN activation leads to a prolonged activation of rhythmic motor activity. This persistent activation of the gastric mill rhythm appears to result from the long-lasting

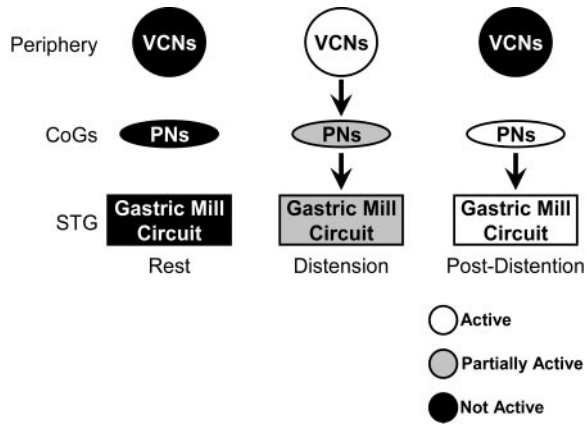

FIG. 13. Working model of the VCN pathway. During rest (i.e., cardiac sac is empty), the VCN pathway is not activated and, consequently, it does not activate CoG projection neurons (PNs). Thus the gastric mill circuit is off. Because the VCN pathway is activated by mechanical pressure, we postulate that the introduction of food to the food-storing cardiac sac distends this foregut compartment and activates the VCN pathway. Because inconsistent or no gastric mill rhythm is recorded during VCN stimulation, the circuit is not coherently activated during cardiac sac distention. Later, once food has moved from the cardiac sac to the gastric mill for chewing, particular CoG projection neurons show regular and persistent activity and therefore the gastric mill rhythm is elicited.

activation of CoG projection neurons, including MCN1 and CPN2. The extended activation of projection neurons by the VCNs is likely to result from a modulatory action, but it is unresolved whether that action comes directly from the VCN neurons. However, consistent with this possibility is the presence of a long-lasting component to the apparently monosynaptic EPSPs from VCN to MCN1, MCN7, and CPN2. Several other identified sensory neurons in the STNS have actions that are likely to be modulatory in nature (Combes et al. 1999; Hooper et al. 1990; Katz and Harris-Warrick 1989, 1990; Meyrand et al. 1994; Robertson and Laverack 1979; Sigvardt and Mulloney 1982; Simmers and Moulins 1988a,b). The modulatory actions of the VCNs are particularly reminiscent of those of a population of about 180 mechanoreceptive neurons, documented in the lobster (*Homarus americanus*, *Palinurus vulgaris*, *Jasus lalandii*), called the posterior stomach receptors (PSRs) (Nagy and Moulins 1981; Selverston and Moulins 1987). The PSRs have long-lasting actions on a subset of pyloric neurons and can activate the gastric mill circuit by exciting CoG projection neurons. Despite having very similar actions, the VCNs and PSRs reside in different regions of the foregut (Dando and Laverack 1969).

The STNS sensory neurons with the most extensively documented modulatory actions are the gastropyloric receptor neurons (GPRs) (Katz and Harris-Warrick 1989, 1990; Katz et al. 1989). One such GPR-elicited action is its modulation of the dorsal gastric (DG) neuron, by its influence on a hyperpolarization-activated inward current (I_h) and a calcium-dependent current, thereby enabling the expression of plateau properties in the DG neuron (Kiehn and Harris-Warrick 1992a,b). Similarly, the transformation of a cutaneous sensory signal into a swim command is also accompanied by the expression of plateau properties in reticulospinal (RS) neurons in the lamprey (Viana di Prisco et al. 1997, 2000). Thus future studies may reveal that VCN activation of the gastric mill circuit is also mediated by the induction of particular membrane properties in upstream CoG projection neurons.

VCN actions on higher-order neurons

The VCN sensory system belongs to a growing list of examples of mechanosensory neurons that have network-configuring properties in addition to the correctional, feedback-providing properties classically ascribed to such neurons. Of particular interest to this study is the recent focus on work aimed at achieving a cellular-level understanding of how sensory inputs can initiate and/or terminate entire motor programs. Several examples of sensory activation of motor programs exist. In the leech *Hirudo medicinalis*, for example, activation of pressure and nociception-sensitive sensory neurons excite subesophageal trigger neurons that drive swim-initiating interneurons that, in turn, activate the swim CPG and initiate swimming (Brodfuehrer et al. 1995; Weeks and Kristan 1978). In *Aplysia*, cerebral-to-buccal interneurons (CBIs) are activated by salient sensory stimuli and initiate/drive buccal motor programs underlying feeding behaviors (Rosen et al. 1991, 2000a,b). Primary afferent activation of a command-like interneuron that activates the swim CPG has also been documented in the marine mollusc *Tritonia diomedea* (Frost and Katz 1996). As mentioned above, RS neurons mediate the ability of sensory systems to influence spinal locomotor circuits. One such neuron is the Mauthner cell, the RS neuron in fish and amphibians that elicits an escape swim in response to tactile stimulation (Eaton et al. 2001; Liu and Fetcho 1999; O'Malley et al. 1996). In the lamprey, cutaneous inputs activate long-lasting, Ca^{2+}-sensitive plateau potentials in RS neurons that are accompanied by escape swimming activity (Viana di Prisco et al. 1997, 2000). Afferent activation can also have long-term negative effects on rhythmic behaviors. For example, pressure applied to a cement gland on the head of *Xenopus laevis* activates inhibitory mid-hindbrain RS neurons that in turn inhibit the swim CPG and terminate swimming behavior (Perrins et al. 2002).

Many issues regarding sensory activation of rhythmic motor activity remain unresolved. One such issue involves whether the transformation of a relatively short-duration sensory stimulus into long-lasting motor output commonly results from direct modulatory actions of the sensory neuron(s). In cases where the long-lasting actions do indeed result from direct, sensory-mediated modulation, the range of underlying cellular mechanisms remains to be determined. It is also unclear how incoming sensory information is represented across a population of projection neurons (for review, see Lewis 1999). These and related issues are now amenable to a detailed cellular analysis using the VCN sensory system, given its ability to activate identified projection neurons that initiate the gastric mill motor program, and because of the accessibility and resulting available characterization of many STNS projection and circuit neurons.

ACKNOWLEDGMENTS

We thank S. Hertzberg for participation in some of this work.

GRANTS

This work was supported by National Institute of Neurological Disorders and Stroke Grants NS-42813 and NS-29436 to M. P. Nusbaum and F31-NS-41894 to M. P. Beenhakker.

Present address of D. M. Blitz: Department of Neurobiology, Harvard Medical School, Boston, MA 02115.

REFERENCES

Akay T, Bassler U, Gerharz P, and Buschges A. The role of sensory signals from the insect coxa-trochanta joint in controlling motor activity of the femur-tibia joint. *J Neurophysiol* 85: 594–604, 2001.

Alexandrowitcz JS. Muscle receptor organs in the abdomen of *Homarus vulgaris* and *Palinurus vulgaris*. *Q J Microscop Sci* 92: 163–203, 1951.

Andersson O and Grillner S. Peripheral control of the cat's step cycle. I. Phase dependent effects of ramp-movements of the hip during "fictive locomotion." *Acta Physiol Scand* 113: 89–101, 1981.

Beenhakker MP, Hertzberg S, and Nusbaum MP. Neural network modulation by mechanosensory activation. *Soc Neurosci Abstr* 26: 449, 2000.

Bennet-Clark HC. Abdominal stretch and inhibition of moulting in *Rhodnius prolixus* (hemiptera). *J Insect Physiol* 12: 1019–1028, 1966.

Blitz DM, Christie AE, Coleman MJ, Norris BJ, Marder E, and Nusbaum MP. Different proctolin neurons elicit distinct motor patterns from a multifunctional neuronal network. *J Neurosci* 19: 5449–5463, 1999.

Blitz DM and Nusbaum MP. Motor pattern selection via inhibition of parallel pathways. *J Neurosci* 17: 4965–4975, 1997.

Blitz DM and Nusbaum MP. Distinct functions for cotransmitters mediating motor pattern selection. *J Neurosci* 19: 6774–6783, 1999.

Boothby KM and Roberts A. The stopping response of *Xenopus laevis* embryos: pharmacology and intracellular physiology of rhythmic spinal neurones and hindbrain neurones. *J Exp Biol* 169: 65–86, 1992.

Brodfuehrer PD, Debski EA, O'Gara BA, and Friesen WO. Neuronal control of leech swimming. *J Neurobiol* 27: 403–418, 1995.

Chiang RG, Chiang JA, and Davey KG. Structure of the abdominal receptor responsive to internally applied pressure in the blood-feeding insect, *Rhodnius prolixus. Cell Tissue Res* 261: 583–587, 1990.

Chiang RG and Davey KG. A novel receptor capable of monitoring applied pressure in the abdomen of an insect. *Science* 241: 1665–1667, 1988.

Clemens S, Combes D, Meyrand P, and Simmers J. Long-term expression of two interacting motor pattern-generating networks in the stomatogastric system of freely behaving lobster. *J Neurophysiol* 79: 1396–1408, 1998.

Coleman MJ and Nusbaum MP. Functional consequences of compartmentalization of synaptic input. *J Neurosci* 14: 6544–6552, 1994.

Coleman MJ, Nusbaum MP, Cournil I, and Claiborne BJ. Distribution of modulatory inputs to the stomatogastric ganglion of the crab, *Cancer borealis. J Comp Neurol* 325: 581–594, 1992.

Combes D, Meyrand P, and Simmers J. Dynamic restructuring of a rhythmic motor program by a single mechanoreceptor neuron in lobster. *J Neurosci* 19: 3620–3628, 1999.

Combes D, Simmers AJ, and Moulins M. Structural and functional characterization of a muscle tendon proprioceptor in lobster. *J Comp Neurol* 363: 221–234, 1995.

Cropper EC, Evans CG, and Rosen SC. Multiple mechanisms for peripheral activation of the peptide-containing radula mechanoafferent neurons B21 and B22 of *Apylsia. J Neurophysiol* 76: 1344–1351, 1996.

Dando MR and Maynard DM. The sensory innervation of the foregut of *Panularis argus* (Decapoda Crustacea). *Mar Behav Physiol* 2: 283–305, 1974.

Duysens J, Clarac F, and Cruse H. Load-regulating mechanisms in gait and posture: comparative aspects. *Physiol Rev* 80: 83–133, 2000.

Duysens J and Pearson KG. Inhibition of flexor burst generation by loading ankle extensor muscles in walking cats. *Brain Res* 187: 321–332, 1980.

Eaton RC, Lee RKK, and Foreman MB. The Mauthner cell and other identified neurons of the brainstem escape network of fish. *Prog Neurobiol* 63: 467–484, 2001.

Evans CG, Alexeeva V, Rybak J, Karhunen T, Weiss KR, and Cropper EC. A pair of reciprocally inhibitory histaminergic sensory neurons are activated within the same phase of ingestive motor programs in *Aplysia. J Neurosci* 19: 845–858, 1999.

Evans CG and Cropper EC. Proprioceptive input to feeding motor programs in *Aplysia. J Neurosci* 18: 8016–8031, 1998.

Frost WN and Katz PS. Single neuron control over a complex motor program. *Proc Natl Acad Sci USA* 93: 422–426, 1996.

Gelperin A. Stretch receptors in the foregut of the blowfly. *Science* 157: 208–210, 1967.

Harris-Warrick RM, Marder E, Selverston AI, and Moulins M. *Dynamic Biological Networks. The Stomatogastric Nervous System*. Cambridge, MA: MIT Press, 1992, p. 328.

Harris-Warrick RM and Sparks DL. Neural control. *Curr Opin Neurobiol* 5: 721–726, 1995.

Hess D and Buschges A. Role of proprioceptive signals from an insect femur-tibia joint in patterning motorneuronal activity of an adjacent leg joint. *J Neurophysiol* 81: 1856–1865, 1999.

Hiebert GW, Whelan PJ, Prochazka A, and Pearson KG. Contribution of hind limb flexor muscle afferents to the timing of phase transitions in the cat step cycle. *J Neurophysiol* 75: 1126–1137, 1996.

Hooper SL, Moulins M, and Nonnotte L. Sensory input induces long-lasting changes in the output of the lobster pyloric network. *J Neurophysiol* 64: 1555–1573, 1990.

Katz PS, Eigg MH, and Harris-Warrick RM. Serotonergic/cholinergic muscle receptor cells in the crab stomatogastric nervous system. I. Identification and characterization of the gastropyloric receptor cells. *J Neurophysiol* 62: 558–570, 1989.

Katz PS and Harris-Warrick RM. Serotonergic/cholinergic muscle receptor cells in the crab stomatogastric nervous system. II. Rapid nicotinic and prolonged modulatory effects on neurons in the stomatogastric ganglion. *J Neurophysiol* 62: 571–581, 1989.

Katz PS and Harris-Warrick RM. Neuromodulation of the crab pyloric central pattern generator by serotonergic/cholinergic proprioceptive afferents. *J Neurosci* 10: 1495–1512, 1990.

Kiehn O and Harris-Warrick RM. 5-HT modulation of hyperpolarization-activated inward current and calcium-dependent outward current in a crustacean motor neuron. *J Neurophysiol* 68: 496–508, 1992a.

Kiehn O and Harris-Warrick RM. Serotonergic stretch receptors induce plateau properties in a crustacean motor neuron by a dual-conductance mechanism. *J Neurophysiol* 68: 485–495, 1992b.

Lam T and Pearson KG. Proprioceptive modulation of hip flexor activity during the swing phase of locomotion in decerebrate cats. *J Neurophysiol* 86: 1321–1332, 2001.

Lewis JE. Sensory processing and the network mechanisms for reading neuronal population codes. *J Comp Physiol A Sens Neural Behav Physiol* 185: 373–378, 1999.

Liu KS and Fetcho JR. Laser ablations reveal functional relationships of segmental hindbrain neurons in zebrafish. *Neuron* 23: 325–335, 1999.

Marder E and Calabrese RL. Principles of rhythmic motor pattern generation. *Physiol Rev* 76: 687–717, 1996.

Marder E and Paupardin-Tritsch D. The pharmacological properties of some crustacean neuronal acetylcholine, gamma-aminobutyric acid and l-glutamate responses. *J Physiol* 280: 213–236, 1978.

Marder E and Pearson KG. Motor control from molecules to bedside. *Curr Opin Neurobiol* 8: 693–696, 1998.

McCrea DA. Neuronal basis of afferent-evoked enhancement of locomotor activity. *Ann NY Acad Sci* 860: 216–225, 1998.

McIver SB. Mechanoreception. In: *Comprehensive Insect Physiology, Biochemistry and Pharmacology. Nervous System: Sensory*, edited by Kerkut GA and Gilbert LI. Oxford, UK: Pergamon Press, 1985, vol. 6, p. 71–132.

Mellen NM and Feldman JL. Phasic vagal sensory feedback transforms respiratory neuron activity *in vitro. J Neurosci* 21: 7363–7371, 2001.

Meyrand P, Simmers J, and Moulins M. Dynamic construction of a neural network from multiple pattern generators in the lobster stomatogastric nervous system. *J Neurosci* 14: 630–644, 1994.

Miller MW, Vu ET, and Krasne FB. Cholinergic transmission at the first synapse of the circuit mediating the crayfish lateral giant escape reaction. *J Neurophysiol* 68: 2174–2184, 1992.

Mohl B. The control of foregut movements by the stomatogastric nervous system in the European house cricket *Acheta domesticus* L. *J Comp Physiol* 80: 1–28, 1972.

Nagy F and Moulins M. Proprioceptive control of the bilaterally organized rhythmic activity of the oesophageal neuronal network in the cape lobster *Jasus lalandii. J Exp Biol* 90: 231–251, 1981.

Norris BJ, Coleman MJ, and Nusbaum MP. Recruitment of a projection neuron determines gastric mill motor pattern selection in the stomatogastric nervous system of the crab, *Cancer borealis*. *J Neurophysiol* 72: 1451–1463, 1994.

Norris BJ, Coleman MJ, and Nusbaum MP. Pyloric motor pattern modification by a newly identified projection neuron in the crab stomatogastric nervous system. *J Neurophysiol* 75: 97–108, 1996.

Nusbaum MP and Beenhakker MP. A small-systems approach to motor pattern generation. *Nature* 417: 343–350, 2002.

Nusbaum MP, Blitz DM, Swensen AM, Wood D, and Marder E. The roles of co-transmission in neural network modulation. *Trends Neurosci* 24: 146–154, 2001.

O'Malley DM, Kao Y-H, and Fetcho JR. Imaging the functional organization of zebrafish hindbrain segments during escape behaviors. *Neuron* 17: 1145–1155, 1996.

Orlov J. Die innervation des darmes der insekten; larven von lamellicorniern. *J Z Wiss Zool* 122: 425–502, 1924.

Orlov J. Uber den histologischen bau des ganglions des mundmagennervensystems der insekten. *Z Mikrosk Anat Forsch* 2: 39–110, 1925.

Pearson K. Could enhanced reflex function contribute to improving locomotion after spinal cord repair? *J Physiol* 533: 75–81, 2001.

Pearson K, Misiaszek JE, and Fouad K. Enhancement and resetting of locomotor activity by muscle afferents. *Ann NY Acad Sci* 860: 203–215, 1998.

Pearson KC and Wolf H. Comparison of motor patterns in the intact and deafferented flight system of the locust. I. Electromyographic analysis. *J Comp Physiol A Sens Neural Behav Physiol* 160: 259–268, 1987.

Pearson KG. Proprioceptive regulation of locomotion. *Curr Opin Neurobiol* 5: 786–791, 1995.

Pearson KG, Reye DN, and Robertson RM. Phase-dependent influences of wing stretch receptors on flight rhythm in the locust. *J Neurophysiol* 49: 1168–1181, 1983.

Pearson KG and Wolf H. Connections of hindwing tegulae with flight neurones in the locust, *Locusta migratoria. J Exp Biol* 135: 381–409, 1988.

Perrins R, Walford A, and Roberts A. Sensory activation and role of inhibitory reticulospinal neurons that stop swimming in hatchling frog tadpoles. *J Neurosci* 22: 4229–4240, 2002.

Rice M. Cibarial stretch receptors in the tsetse fly (*Glossina austeni*) and the blowfly (*Calliphora erythrocephala*). *J Insect Physiol* 16: 277–289, 1970.

Ringel M. Zur morphologie des vorderdarmes (schund und magen) von *Astacus fluviatilis. Z Wiss Zool* 123: 498–554, 1924.

Robertson RM and Laverack MS. Oesophageal sensors and their modulatory influence on oesophageal peristalsis in the lobster, *Homarus gammarus. Proc R Soc Lond B Biol Sci* 206: 235–263, 1979.

Rosen SC, Miller MW, Cropper EC, and Kupfermann I. Outputs of radula mechanoafferent neurons in *Aplysia* are modulated by motor neurons, interneurons, and sensory neurons. *J Neurophysiol* 83: 1621–1636, 2000a.

Rosen SC, Miller MW, Evans CG, Cropper EC, and Kupfermann I. Diverse synaptic connections between peptidergic radula mechanoafferent neurons and neurons in the feeding system of *Aplysia. J Neurophysiol* 83: 1605–1620, 2000b.

Rosen SC, Teyke T, Miller MW, Weiss KR, and Kupfermann I. Identification and characterization of cerebral-to-buccal interneurons implicated in the control of motor programs associated with feeding in *Aplysia. J Neurosci* 11: 3630–3655, 1991.

Selverston AI and Moulins M. *The Crustacean Stomatogastric System*. Berlin: Springer-Verlag, 1987, p. 338.

Sigvardt KA and Mulloney B. Sensory alteration of motor patterns in the stomatogastric nervous system of the spiny lobster *Panulirus interruptus. J Exp Biol* 97: 137–152, 1982.

Simmers J and Moulins M. A disynaptic sensorimotor pathway in the lobster stomatogastric system. *J Neurophysiol* 59: 740–756, 1988a.

Simmers J and Moulins M. Nonlinear interneuronal properties underlie integrative flexibility in a lobster disynaptic sensorimotor pathway. *J Neurophysiol* 59: 757–777, 1988b.

Stein PSG, Grillner S, Selverston AI, and Stuart DG. *Neurons, Networks, and Motor Behavior*. Cambridge, MA: The MIT Press, 1997, p. 305.

Sugawara T. Oviposition behaviour of the cricket *Teleogryllus commodus*: mechanosensory cells in the genital chamber and their role in the switch-over of steps. *J Insect Physiol* 39: 335–346, 1993.

Sugawara T. Chordotonal sensilla embedded in the epidermis of the soft integument of the cricket, *Teleogryllus commodus. Cell Tissue Res* 284: 125–142, 1996.

Sugawara T and Loher W. Oviposition behaviour of the cricket *Teleogryllus commodus*: observation of external and internal events. *J Insect Physiol* 32: 179–188, 1986.

Viana di Prisco G, Pearlstein E, Le Ray D, Robitaille R, and Dubuc R. A cellular mechanism for the transformation of a sensory input into a motor command. *J Neurosci* 20: 8169–8176, 2000.

Viana di Prisco G, Pearlstein E, Robitaille R, and Dubuc R. Role of sensory-evoked NMDA plateau potentials in the initiation of locomotion. *Science* 278: 1122–1125, 1997.

Wales W, Clarac F, Dando MR, and Laverack MS. Innervation of the receptors present at the various joints of the pereiopods and third maxilliped of *Homarus gammarus* (L.) and other macruran decapods (Crustacea). *Z vergl Physiol* 68: 345–384, 1970.

Wallen P. Spinal mechanisms controlling locomotion in dogfish and lamprey. *Acta Physiol Scand Suppl* 503: 3–45, 1982.

Weeks JC and Kristan WB Jr. Initiation, maintenance and modulation of swimming in the medicinal leech by the activity of a single neurone. *J Exp Biol* 77: 71–88, 1978.

Weimann JM and Marder E. Switching neurons are integral members of multiple oscillatory networks. *Curr Biol* 4: 896–902, 1994.

Whelan PJ, Hiebert GW, and Pearson KG. Stimulation of the group I extensor afferents prolongs the stance phase in walking cats. *Exp Brain Res* 103: 20–30, 1995.

Wilson D. The central nervous control of locust flight. *J Exp Biol* 38: 471–490, 1961.

Wolf H and Pearson KG. Comparison of motor patterns in the intact and deafferented flight systems of the locust. *J Comp Physiol A Sens Neural Behav Physiol* 160: 269–279, 1987.

Wolf H and Pearson KG. Proprioceptive input patterns elevator activity in the locust flight system. *J Neurophysiol* 59: 1831–1853, 1988.

Wood DE and Nusbaum MP. Extracellular peptidase activity tunes motor pattern modulation. *J Neurosci* 22: 4185–4195, 2002.

Wood DE, Stein W, and Nusbaum MP. Projection neurons with shared cotransmitters elicit different motor patterns from the same neuronal circuit. *J Neurosci* 20: 8943–8953, 2000.